Structure and organization of the human antimicrobial peptide LL-37 in phospholipid membranes: relevance to the molecular basis for its non-cell-selective activity

Ziv OREN*, Jeffrey C. LERMAN*, Gudmundur H. GUDMUNDSSON†, Birgitta AGERBERTH‡ and Yechiel SHAI*[1]

*Department of Biological Chemistry, The Weizmann Institute of Science, Rehovot 76100, Israel, †Microbiology and Tumorbiology Center, Karolinska Institute, S-17177 Stockholm, Sweden, and ‡Department of Medical Biochemistry and Biophysics, Karolinska Institute, S-17177 Stockholm, Sweden

The antimicrobial peptide LL-37 belongs to the cathelicidin family and is the first amphipathic α-helical peptide isolated from human. LL-37 is considered to play an important role in the first line of defence against local infection and systemic invasion of pathogens at sites of inflammation and wounds. Understanding its mode of action may assist in the development of antimicrobial agents mimicking those of the human immune system. *In vitro* studies revealed that LL-37 is cytotoxic to both bacterial and normal eukaryotic cells. To gain insight into the mechanism of its non-cell-selective cytotoxicity, we synthesized and structurally and functionally characterized LL-37, its N-terminal truncated form FF-33, and their fluorescent derivatives (which retained structure and activity). The results showed several differences, between LL-37 and other native antimicrobial peptides, that may shed light on its *in vivo* activities. Most interestingly, LL-37 exists in equilibrium between monomers and oligomers in solution at very low concentrations. Also, it is significantly resistant to proteolytic degradation in solution, and when bound to both zwitterionic (mimicking mammalian membranes) and negatively charged membranes (mimicking bacterial membranes). The results also showed a role for the N-terminus in proteolytic resistance and haemolytic activity, but not in antimicrobial activity. The LL-37 mode of action with negatively charged membranes suggests a detergent-like effect via a 'carpet-like' mechanism. However, the ability of LL-37 to oligomerize in zwitterionic membranes might suggest the formation of a transmembrane pore in normal eukaryotic cells. To examine this possibility we used polarized attenuated total reflectance Fourier-transform infrared spectroscopy and found that the peptide is predominantly α-helical and oriented nearly parallel with the surface of zwitterionic-lipid membranes. This result does not support the channel-forming hypothesis, but rather it supports the detergent-like effect.

Key words: amphipathic helix, antimicrobial peptide, cathelicidin, innate immunity, LL-37.

INTRODUCTION

Peptide antibiotics constitute a major part of the innate immunity of groups as diverse as plants, invertebrates and vertebrates including humans [1,2]. This defence system is composed of distinct groups of broad-spectrum antimicrobial peptides that act alongside of the highly specific cell-mediated immune system. Cathelin is a putative cysteine-proteinase inhibitor, first isolated from pig leucocytes [3], which has now also been found to constitute a proregion for many different peptide antibiotics [4]. The cathelicidin-protein family, now counting more than 20 members, constitutes a significant part of mammalian peptide antibiotics in a variety of species including cow, pig, sheep, rabbit, mouse and, recently, humans [4–12]. Most of the cathelicidin precursors are stored in cytoplasmic granules of neutrophil leucocytes and release the antimicrobial peptides upon leucocyte activation [13,14]. Members of the cathelicidin family have various structures and different killing mechanisms. For example, PMAP-36 [15], PMAP-37 [16], CRAMP [11], BMAP-27 and BMAP-28 [17] adopt a predominantly α-helical structure, and rapidly permeabilize the bacterial membrane. Others, which do not adopt an α-helical structure, like Bac5 and Bac7, inhibit incorporation of precursor molecules into protein and RNA [18], while PR-39 stops protein and DNA synthesis in Gram-negative bacteria [19].

The human LL-37 (two-amino-acid-truncated form of FALL-39 [12]) belongs to the cathelicidin family [20]. The peptide has also been named hCAP18 [21]. FALL-39 was first identified as a putative antimicrobial peptide in a cDNA clone isolated from a human-bone-marrow library [12]. It was expressed in bone marrow and testes, but not in 15 other human tissues tested. The gene has been mapped to chromosome 3 in humans [22], and synthetic FALL-39 was biologically active. Wheel projection indicated that FALL-39 can form an amphipathic α-helical structure, a common motif in lytic peptides [23]. Indeed, circular dichroism measurements demonstrated that the peptide adopts an α-helical structure in a physiological salt medium (medium E) [12]. The complete gene for FALL-39 (CAMP or cathelicidin antimicrobial peptide) was recently characterized [20]. LL-37 was isolated from human granulocytes and sequence analysis

Abbreviations used: Boc, *t*-butoxycarbonyl; CFU, colony-forming units; diS-C_2-5, 3,3′-diethylthiodicarbocyanine iodode; EDC, 1-ethyl-3-(3-dimethylaminopropyl)carbodi-imide hydrochloride; hRBC, human red blood cells; MIC, minimal inhibitory concentration; NBD-F, 4-fluoro-7-nitrobenz-2-oxa-1,3-diazole; PC, egg phosphatidylcholine; PS, phosphatidylserine; PG, egg phosphatidylglycerol; RET, resonance energy transfer; Rho, carboxytetramethylrhodamine succinimidyl ester; SUV, small unilamellar vesicles; TFA, trifluoroacetic acid; ATR, attenuated total reflectance; FTIR, Fourier-transform infrared.

[1] To whom correspondence should be addressed (e-mail bmshai@weizmann.weizmann.ac.il).

indicated that it corresponded to residues 3–39 of FALL-39 [20]. LL-37 has the following sequence:

LLGDFFRKSKEKIGKEFKRIVQRIKDFLRNLVPRTES

LL-37 was detected in human wounds and blister fluids [24], and more recently the gene coding for LL-37 was found to be induced in human keratinocytes during inflammatory disorders [25]. These findings suggest an important role for LL-37 in the first line of defense against local infection and systemic invasion of pathogens at sites of inflammation and wound. In addition, LL-37 is the first α-helical antimicrobial peptide isolated from a human source. Whereas most known antimicrobial peptides (e.g. cecropin, magainin, dermaseptin) are cytotoxic to several microorganisms, but not to normal eukaryotic cells, LL-37 exhibits cytotoxic activity also to eukaryotic cells [26]. To investigate the molecular basis for the non-cell-selective cytotoxic activity of LL-37, the peptide and its N-terminal-truncated form were synthesized and fluorescently labelled. The peptides were then characterized with respect to their structure, ability to interact with membranes, cytotoxicity against bacteria and human erythrocytes, as well as their organization and resistance to proteolysis. The results are discussed in terms of a proposed model for the mode of action of LL-37.

EXPERIMENTAL

Materials

t-Butoxycarbonyl- (Boc-) amino acids were obtained from Peninsula Laboratories (Belmont, CA, U.S.A.), *N*-Boc-*O*-*p*-bromobenzyloxycarbonylserine phenylacetamidomethyl ester resin was purchased from Applied Biosystems (Foster City, CA, U.S.A.). Other reagents used for peptide synthesis included trifluoroacetic acid (TFA from Sigma, *N*,*N*-di-isopropylethylamine (Aldrich), dicyclohexylcarbodi-imide (Fluka), 1-hydroxybenzotriazole (Pierce) and peptide-synthesis grade dimethylformamide (Biolab, Jerusalem, Israel). Egg phosphatidylcholine (PC) and phosphatidylserine (PS) from bovine spinal cord (sodium salt, grade I) were purchased from Lipid Products (South Nutfield, Redhill, Surrey, U.K.). Egg phosphatidylglycerol (PG) was purchased from Sigma. Cholesterol (extra pure) was supplied by Merck and recrystallized twice from ethanol. 3,3′-Diethylthiodicarbocyanine iodide (diS-C_2-5) and 5-(and-6)-carboxytetramethylrhodamine succinimidyl ester (Rho) were obtained from Molecular Probes (Eugene, OR, U.S.A.). 4-Fluoro-7-nitrobenz-2-oxa-1,3-diazole (NBD-F) was obtained from Sigma. 1-Ethyl-3-(3-dimethylaminopropyl)-carbodiimide hydrochloride (EDC) was purchased from Pierce, and *N*-hydroxysuccinimide was obtained from Sigma. Buffers were prepared in double glass-distilled water.

Synthesis, fluorescent labelling and purification of peptides

Peptides were synthesized by a solid phase method on *N*-Boc-*O*-*p*-bromobenzyloxycarbonylserine phenylacetamidomethyl ester resin [27]. Labelling of the N-terminus of LL-37 with fluorescent probes was achieved by labelling the resin-bound peptide as previously described [28]. Briefly, 10–30 mg of resin-bound peptide were treated with TFA (50 %, v/v, in methylene chloride), to remove the Boc protecting group from the N-terminus of the linked peptide. The resin-bound peptide was then allowed to react with either (i) carboxytetramethylrhodamine succinimidyl ester (3–4 equiv.) in dry dimethylformamide containing 5 % (v/v) di-isopropylethylamine, or (ii) NBD-F (2 equiv.) in dry dimethylformamide. The resin-bound peptides were cleaved from the resins with HF, and finally extracted with dry diethyl ether after HF evaporation. The synthetic peptides were further purified by reverse-phase HPLC on a C_{18} reverse-phase Bio-Rad semi-preparative column (10 mm × 250 mm, 300 Å pore size, 5 μm particle size). The column was eluted in 40 min, using a linear gradient of 15–80 % (v/v) acetonitrile in water, both containing 0.05 % TFA (v/v), at a flow rate of 1.8 ml/min. The purified peptides were shown to be homogeneous (~ 98 %) by analytical HPLC. The peptides were subjected to amino-acid analysis to confirm their composition. The molecular mass was determined by matrix-assisted laser desorption ionization–time-of-flight MS (Lasermat 2000, from Finnigan Mat, Bremen, Germany) and agreed with the calculated mass.

Preparation of Liposomes

Small unilamellar vesicles (SUV) were prepared by sonication of PC/cholesterol (10:1, w/w) or PC/PS (1:1, w/w) dispersions. Briefly, dry lipids and cholesterol (10:1, w/w) were dissolved in a chloroform/methanol mixture (2:1, v/v). The solvents were evaporated under a stream of nitrogen and the lipids were subjected to a vacuum for 1 h and then resuspended (at a concentration of 7.2 mg/ml) in the appropriate buffer by vortexing. The resultant lipid dispersions were then sonicated for 5–15 min in a bath-type sonicator (model G1125SP1 sonicator, Laboratory Supplies Company Inc., New York, NY, U.S.A.) until clear. The lipid concentrations of the resulting preparations were determined by phosphorus analysis [29]. Vesicles were visualized using a JEOL JEM 100B electron microscope (Japan Electron Optics Laboratory Co., Tokyo, Japan) as follows. A drop of vesicles was deposited on a carbon-coated grid and negatively stained with uranyl acetate. Examination of the grids demonstrated that the vesicles were unilamellar with an average diameter of 20–50 nm.

Antimicrobial activity of the peptides

The antimicrobial activity of the peptides was examined in sterile 96-well plates (Nunc F96 microtitre plates) in a final volume of 100 μl as follows: aliquots (50 μl) of a suspension containing bacteria at a concentration of 1×10^6 colony-forming units (CFU)/ml in Lurie–Bertani culture medium were added to 50 μl of water, containing the peptide in serial 2-fold dilutions. Inhibition of growth was determined by measuring the attenuance at 492 nm with a Microplate Autoreader E1309 (Bio Tek Instruments, Winooski, VT, U.S.A.), after an incubation time of 18–20 h at 37 °C. Antimicrobial activities were expressed as the minimal inhibitory concentration (MIC), the concentration at which 100 % inhibition of growth was observed after 18–20 h of incubation. The bacteria used were: *Escherichia coli* D21, a Gram-negative bacteria, and *Bacillus megaterium* Bm11, a Gram-positive bacteria.

Haemolysis of human red blood cells

The haemolytic activity of the peptides and their fluorescent derivatives was tested against human red blood cells (hRBC). Fresh hRBC with EDTA (2 mg/ml) were rinsed three times with PBS (35 mM phosphate buffer/0.15 M NaCl, pH 7.3) by centrifugation for 10 min at 800 ***g*** and resuspended in PBS. Peptides, dissolved in PBS, were then added to 50 μl of a solution of the stock hRBC in PBS to reach a final volume of 100 μl (final hRBC concentration, 5 %, v/v). The resulting suspension was incubated with agitation for 1 h at 37 °C. The samples were then centrifuged at 800 ***g*** for 10 min. Release of haemoglobin was monitored by

measuring the absorbance of the supernatant at 540 nm. Controls for zero haemolysis (blank) and 100% haemolysis consisted of hRBC suspended in PBS and Triton 1% (v/v) respectively.

Oligomerization of the peptides in solution as determined by Rhodamine fluorescence 'Dequenching'

Rhodamine-labelled peptide (0.1 μM final concn.) was added to 2 ml of PBS, and rhodamine fluorescence emission was monitored. Proteinase K (10 μg/ml) was then added, resulting in an increase in the fluorescence emission as a result of the dequenching of the rhodamine fluorescence. More proteinase K was added until no further increase in the fluorescence emission was observed. Excitation was set at 530 nm (10 nm slit) and emission was set at 582 nm (8 nm slit). These and all subsequent fluorescence measurements were performed at room temperature on a Perkin–Elmer LS-50B spectrofluorimeter, equipped with a magnetic stirrer.

Chemical cross-linking of LL-37 oligomers in solution

Reaction mixtures were composed of 20 μg of LL-37 dissolved in 50 mM potassium phosphate (pH 8.1) at final concentrations of 0.5 μM, 1.5 μM and 50 μM LL-37. The reaction was initiated by addition of the cross-linker (0.7 mM final concn.) in the presence of *N*-hydroxysuccinimide (0.1 mM final concn.). After 3 h incubation at room temperature (22–25 °C), the unreacted cross-linker was removed by gel filtration through a 1 ml Sephadex G-50 mini-column. The resulting cross-linked complexes ($\sim$ 20 μg each) were lyophilized, resuspended in 50 μl of 50 mM KP_i (pH 8.1), and equal amounts of each peptide ($\sim$ 2 μg, 5 μl) were resolved by SDS/15% (w/v) PAGE and stained with Coomassie Blue as described in [30]. Fixing, staining, and destaining times were shortened to 1 min, 1 h, and overnight, respectively, so that diffusion effects were minimized.

NBD fluorescence measurements

NBD-labelled peptide (0.2 nmol) was added to 2 ml of PBS, pH 7.3, containing 600 nmol of PC SUV or PS/PC SUV, to establish a lipid/peptide ratio of 3000:1, in which all the peptide is bound to lipids. After a 20 min incubation, the emission spectrum of the NBD group was recorded (3 separate experiments) with the excitation set at 470 nm (10 nm slit).

Membrane permeation induced by the peptides

Membrane permeation was assessed utilizing the diffusion-potential assay as previously described [31]. In a typical experiment, 4 μl of a liposome suspension (32 μM final concentration), prepared in a K^+-containing buffer (50 mM K_2SO_4/25 mM Hepes/SO_4^{2-}, pH 6.8), were diluted in 1 ml of an isotonic K-free buffer (50 mM Na_2SO_4/25 mM Hepes/SO_4^{2-}, pH 6.8) in a glass tube. To this solution the fluorescent potential-sensitive dye, diS-C_2-5 was then added. Valinomycin (1 μl of a 10^{-7} M stock solution) was added to the suspension to slowly create a negative diffusion potential inside the vesicles, which led to a quenching of the dye's fluorescence. Once the fluorescence had stabilized, 3–10 min later, peptides were added. The subsequent dissipation of the diffusion potential, as reflected by an increase in fluorescence, was monitored with excitation set at 620 nm and emission set at 670 nm and the gain adjusted to 100%. The percentage of fluorescence recovery, F_t, was defined as:

$$F_t = [(I_t - I_0)/(I_f - I_0)] \times 100$$

where I_0 = the initial fluorescence, I_f = the total fluorescence observed before the addition of valinomycin, and I_t = the fluorescence observed after adding the peptide, at time t.

Accessibility of membrane-bound peptides to proteolytic degradation

Lipid vesicles (150 μM in a 2 ml cuvette) were added to NBD-labelled peptides (0.1 μM, in PBS). After 15 min, proteinase K (10 μg/ml) was added. Fluorescence emission as a function of time was recorded before and after the addition of the enzyme. In control experiments, NBD-labelled peptides were pre-incubated with proteinase K in aqueous solution, followed by the addition of the liposomes. Fluorescence measurements were performed with excitation set at 470 nm (10 nm slit) and emission set at 530 nm (8 nm slit).

Visible attenuance measurements

The changes in the vesicles' size were measured by visible attenuance measurements. Aliquots of peptide stock solutions were added to 200 μl suspensions of 150 μM vesicles SUV composed of either PC/cholesterol (10:1, w/w) or PC/PS (1:1, w/w) in PBS. Attenuance was measured at 405 nm using the Microplate Autoreader before and after the addition of a peptide.

Visualization of vesicle aggregation by electron microscopy

The effects of the peptide on liposomal suspensions were examined by negative-stain electron microscopy. A drop containing PC/cholesterol (10:1, w/w) or PC/PS (1:1, w/w) SUV alone, or a mixture of SUV and a peptide, was deposited onto a carbon-coated grid and negatively stained with phosphotungstic acid, 2% (w/v) pH 6.8. The grids were examined using a JEOL JEM 100B electron microscope.

Resonance energy transfer (RET) measurements

Fluorescence spectra were obtained at room temperature, with the excitation monochromator set at 460 nm (5 nm slit width) to minimize the excitation of tetramethylrhodamine. Measurements were performed in a 1-cm-path-length glass cuvette with a final reaction volume of 2 ml. In a typical experiment, donor (NBD-labelled) peptide at a final concentration of 0.1 μM was added to a dispersion of PC (125 μM) or PC/PS SUV in PBS buffer, followed by the addition of acceptor (Rho-labelled) peptide in several sequential doses. Fluorescence spectra were obtained before and after the addition of the acceptor peptide. Changes in the fluorescence intensity of the donor due to processes other than energy transfer to the acceptor were determined by substituting unlabelled peptide for the acceptor, and by measuring the emission spectrum of the acceptor alone in the presence of vesicles.

Attenuated total reflectance Fourier-transform infrared (ATR-FTIR) spectroscopy

Spectra were obtained with a Bruker Equinox 55 FTIR spectrometer equipped with a [^{2}H]triacylglycerol-sulphate detector and coupled with an ATR device. For each spectrum (resolution 4 cm^{-1}), 200–300 scans were collected. During data acquisition, the spectrometer was continuously purged with dry N_2 to eliminate the spectral contribution of atmospheric water. Samples were prepared as previously described [32]. Briefly, a mixture of PC/cholesterol (10:1, w/w, 1 mg) or PC/PG (1:1, w/w, 1 mg)

alone or with peptide (80 μg) was deposited on a ZnSe horizontal attenuated total reflectance (ATR) prism (80 mm × 7 mm). The aperture angle of 45° yielded 25 internal reflections. Prior to sample preparation, the trifluoroacetate counterions, which strongly associate with the peptides, were replaced with chloride ions through several lyophilizations of the peptides in 0.1 M HCl. This allowed the elimination of the strong C=O stretching absorption band near 1673 cm^{-1} [33]. Lipid/peptide mixtures were prepared by dissolving them together in a methanol/dichloromethane (1:2) mixture and drying under a stream of dry N_2 while moving a teflon bar back and forth along the ZnSe prism. Polarized spectra were recorded and the spectra from the respective pure phospholipids in each polarization were subtracted to yield the difference spectra. The background for each spectrum was a clean ZnSe prism. Hydration of the sample was achieved by introduction of excess of deuterium oxide (^2H_2O) into a chamber placed on top of the ZnSe prism in the ATR casting and subsequent incubation for 2 h prior to acquisition of spectra. $H \leftrightarrow {}^2H$ exchange was considered complete due to the complete shift of the amide II band [34]. Any contribution of ^2H_2O vapours to the absorbance spectra near the amide I peak region was eliminated by subtraction of the spectra of pure lipids equilibrated with ^2H_2O under the same conditions.

ATR-FTIR data analysis

Prior to curve fitting, a straight baseline passing through the ordinates at 1700 cm^{-1} and 1600 cm^{-1} was subtracted. To resolve overlapping bands, the spectra were processed using PEAKFIT™ (Jandel Scientific, San Rafael, CA, U.S.A.) software. Second-derivative spectra accompanied by 13-data-point Savitsky–Golay smoothing were calculated to identify the positions of the components' bands in the spectra. These wavenumbers were used as initial parameters for curve fitting with gaussian component peaks. Position, bandwidths, and amplitudes of the peaks were varied until: (i) the resulting bands shifted by no more than 2 cm^{-1} from the initial parameters, (ii) all the peaks had reasonable half-widths (< 20–25 cm^{-1}), and (iii) good agreement between the calculated sum of all components and the experimental spectra was achieved ($r^2 > 0.99$). The relative contents of different secondary structural elements were estimated by dividing the areas of individual peaks, assigned to particular secondary structure, by the whole area of the resulting amide I band. The results of four independent experiments were averaged.

Analysis of the polarized ATR-FTIR spectra

The ATR electric fields of incident light were calculated as follows [35,36]:

$$E_x = \frac{2\cos\theta\sqrt{\sin^2\theta - n_{21}^2}}{\sqrt{(1-n_{21}^2)[(1+n_{21}^2)\sin^2\theta - n_{21}^2]}}$$

$$E_y = \frac{2\cos\theta}{\sqrt{1-n_{21}^2}}$$

$$E_z = \frac{2\sin\theta\cos\theta}{\sqrt{(1-n_{21}^2)[(1+n_{21}^2)\sin^2\theta - n_{21}^2]}}$$

where θ is the angle of a light beam to the prism normal at the point of reflection (45°), and $n_{21} = n_2/n_1$ [n_1 and n_2 are the refractive indices of ZnSe ($n_1 = 2.4$) and the membrane sample ($n_2 = 1.5$), respectively]. Under these conditions, E_x, E_y and E_z are 1.09, 1.81 and 2.32, respectively. The electric field components together with the dichroic ratio [R^{ATR}, defined as the ratio between absorption of parallel (with a membrane plane), A_p, and perpendicularly polarized incident light, A_s] are used to calculate the orientation order parameter, f, by the following formula:

$$R^{ATR} = \frac{A_p}{A_s} = \frac{E_x^2}{E_y^2} + \frac{\frac{E_z^2}{E_y^2}\left[(f\cos^2\alpha) + \left(\frac{1-f}{3}\right)\right]}{\frac{f\sin^2\alpha}{2} + \frac{1-f}{3}}$$

where α is the angle between the transition moment of the amide I vibration of an α-helix and the helix axis. We used a value of 27° for α, as was previously suggested [36,37]. Lipid-order parameters were obtained from the symmetric (~ 2853 cm^{-1}) and antisymmetric (~ 2922 cm^{-1}) lipid-stretching modes using the same equations, setting $\alpha = 90°$ [36].

Examination of bacterial membrane damage by electron microscopy

Samples containing *E. coli* (1×10^6 CFU/ml) in Lurie–Bertani medium, supplemented with basal medium E, were incubated for 1 h with LL-37, or the antimicrobial peptide cecropin B as a control. The peptides were supplied at their MIC and 60% of their MIC. After centrifuging for 10 min at 3000 ***g*** the pellets were resuspended, and a drop containing the bacteria was deposited on to a carbon-coated grid and negatively stained with phosphotungstic acid, 2% pH 6.8. The grids were examined using a JEOL JEM 100B electron microscope.

RESULTS

Antimicrobial and haemolytic activity of LL-37, FF-33 and their fluorescently labelled analogues

The peptides were studied for their potential to inhibit the growth of Gram-positive and Gram-negative bacteria. The MIC for *E. coli* D21 was the same (12.5–25 μM) for LL-37, FF-33 and their NBD- and Rho-labelled analogues. Similarly, for *B. megaterium* Bm11, all the peptides were equally active, and the MIC was 0.75–1.5 μM.

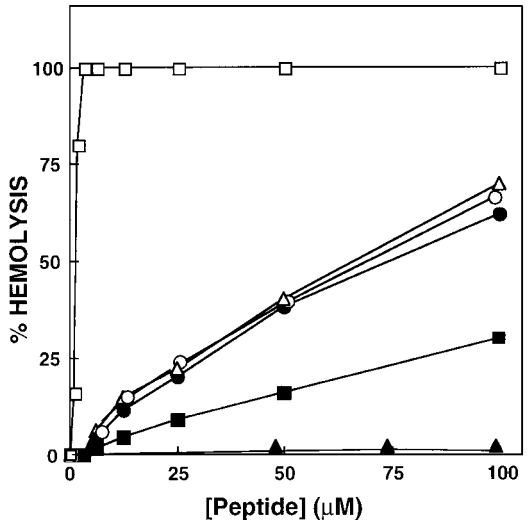

Figure 1 Dose-response curve of the haemolytic activity of the peptides towards hRBC

The assay was performed as described in the Experimental section. Designations: (□), melittin; (●), LL-37; (■), FF-33; (▲), cecropin B; (○), NBD-LL-37; (△), Rho-LL-37.

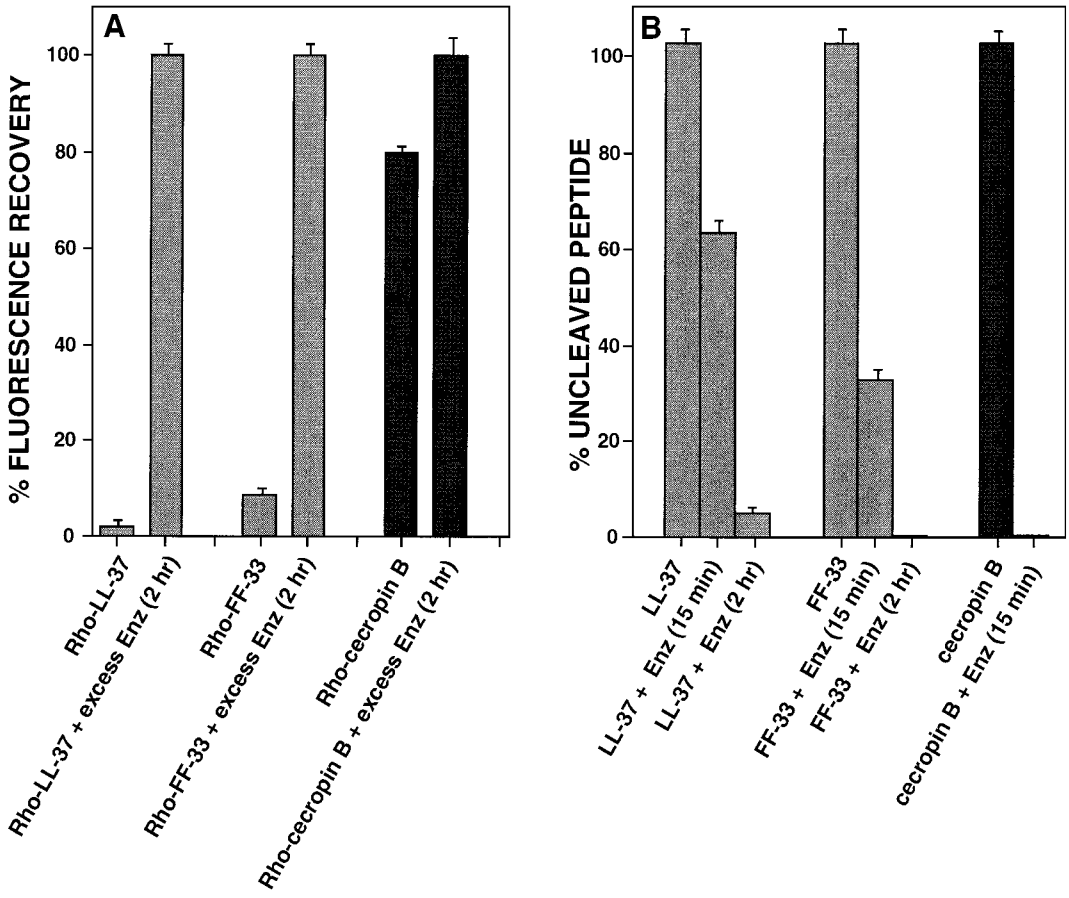

Figure 2 Determination of the aggregation state of LL-37 in solution

(**A**) The percentage of fluorescence recovery of Rho-LL-37 (0.1 μM), Rho-FF-33 (0.1 μM) and Rho-cecropin B (0.1 μM, serving as a control) in PBS in the presence and absence of proteinase K (Enz) at a concentration of 10 μg/ml. Excitation was set at 530 nm (10 nm slit) and emission was set at 582 nm (8 nm slit). (**B**) Enzymic degradation of the peptides. Peptides (80 μg) were treated with proteinase K (7.5 μg/ml) and percentage uncleaved peptide as a function of time was determined by reverse phase-HPLC.

LL-37, FF-33 and their fluorescent derivatives were also tested for their haemolytic activity against the highly susceptible hRBC. Figure 1 shows the dose-response haemolytic activity of all the peptides tested. The effects of melittin and cecropin B are shown for comparison. LL-37 and its fluorescent derivatives had significant haemolytic activity at concentrations which are required for antimicrobial activity, whereas cecropin B is devoid of haemolytic activity at concentrations up to 100 μM (maximum concentration tested). The truncated version FF-33 is about 2-fold less haemolytic than LL-37. Figure 1 shows also that the fluorescent derivatives have a haemolytic activity similar to the unlabelled peptides.

LL-37 self-associates in solution and is more resistant to proteolytic degradation than FF-33

The ability of LL-37 and FF-33 to self-associate in solution was investigated using Rho-labelled peptides. The fluorescence of rhodamine is only slightly sensitive to the polarity of its environment and therefore it can be studied in solution. In addition, the fluorescence of rhodamine is quenched when several molecules are in close proximity; therefore a difference in the fluorescence intensity between a peptide treated with proteolytic enzyme and an untreated peptide indicates whether that peptide is associated in solution or not. In the actual experiment, equal concentrations of Rho-LL-37, Rho-FF-33 and Rho-cecropin B were treated with proteinase K. Figure 2(A) reveals that the initial fluorescence of Rho-LL-37 and Rho-FF-33 are much lower than that of Rho-cecropin B, indicating that they are mainly oligomers in solution. The initial fluorescence of Rho-LL-37 is also less than that of Rho-FF-33, which suggests a higher oligomeric state for LL-37 compared with FF-33. After 4 h of treatment with proteinase K, which resulted in total degradation of the peptides (see below), the fluorescence intensity of all the peptide reached similar values.

The susceptibility of the unlabelled peptides to enzymic degradation was assessed by reverse-phase HPLC. Equal amounts of LL-37, FF-33 and cecropin B were treated with proteinase K, and aliquots were injected on to a C_{18} column after 15, 60 and 120 min. Figure 2(B) shows that LL-37, and to a lesser extent its truncated version FF-33, are significantly protected from degradation compared with cecropin B, which is highly susceptible to degradation.

Oligomerization of LL-37 in solution

The state of aggregation of LL-37 was determined by chemical cross-linking. Best results were obtained with EDC, a potent

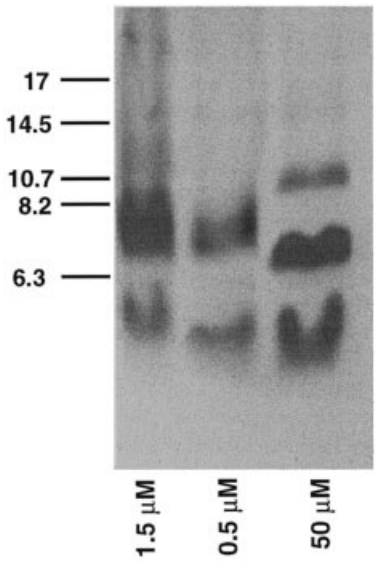

Figure 3 Determination of the oligomerization states of LL-37 in solution, by chemical cross-linking

The Figure shows a Coomassie Blue-stained gel with samples of peptides run on 15% SDS/PAGE. Samples were prepared as described in the Experimental section. LL-37 concentrations used are shown in the Figure, and the numbers beside the gel show the molecular masses of the markers (kDa). LL-37 which was not cross-linked showed predominantly dimers (results not shown).

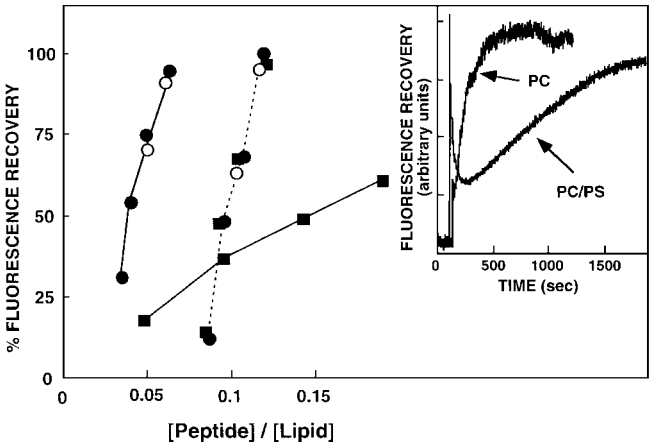

Figure 4 Maximal dissipation of the diffusion potentials in SUV induced by the peptides

The peptide was added to 1 ml of isotonic K^+-free buffer containing a constant concentration (32 μM) of vesicles composed of PS/PC (dotted line) or PC (continuous line), pre-equilibrated with the fluorescent dye [diS-C_2-5] and valinomycin. The maximum fluorescence recovery is plotted as a function of the peptide/lipid molar ratio. Designations: (●), LL-37; (■), FF-33; (○), Rho-LL-37. The activity of the other labelled peptides was similar to that of the parent unlabelled peptides and therefore not shown. (*Inset*) Kinetics of fluorescence recovery after the addition of LL-37 to PC or PS/PC at similar levels of activity. Peptide/lipid molar ratios are 0.044 and 0.11 for PC and PC/PS, respectively.

carboxy-to-amino-group cross-linker. As shown in Figure 3, at LL-37 concentrations of 0.5 μM and 1.5 μM equilibrium exists between monomer and dimer whereas at a higher concentration (50 μM) trimers were also observed.

LL-37 and FF-33 are equally potent in permeating negatively charged but not zwitterionic-phospholipid membranes

Model phospholipid membranes were used to find out whether the non-cell-selective activity of LL-37 resides from its inability to discriminate between negatively charged membranes (the major component of the bacterial outer wall) and zwitterionic membranes (the major component of the outer surface of normal eukaryotic cells). LL-37, FF-33 and their fluorescent derivatives were examined for their efficacy in perturbing the lipid packing and causing leakage of vesicular contents at physiological pH, by utilizing the dissipation-of-diffusion-potential assay. Increasing concentrations of peptides were mixed either with PC or with PC/PS SUV that had been pretreated with the fluorescent, potential-sensitive dye (diS-C_2-5) and valinomycin. Recovery of fluorescence was monitored as a function of time. Maximal activity of LL-37 and its analogues was plotted versus peptide/lipid molar ratios and is shown in Figure 4. Each point is the mean for three separate experiments with an S.D. of $\sim 5\%$. The activity of the fluorescently-labelled analogues was identical with that of the parent peptides and therefore only few points are shown. The results revealed that LL-37 and FF-33 permeated efficiently both PC and PC/PS vesicles. This is in contrast with the very low level of activity observed for PC vesicles with non-haemolytic α-helical antimicrobial peptides, e.g. magainin, cecropin, dermaseptins [28,38–40]. Furthermore, whereas LL-37 and FF-33 are equally active on PC/PS vesicles, LL-37 is more active than FF-33 on PC vesicles. These results correlate with the identical anti-microbial activities expressed by the two peptides and the higher haemolytic activity of LL-37 compared with FF-33. The results also revealed that the kinetics of the permeation process is much slower with PC/PS than with PC, when compared at similar activity (inset of Figure 4). Similar kinetics were observed with FF-33 (results not shown). A possible explanation for this behaviour relates to the difference in the organization of the peptides in both types of vesicles. As will be discussed in the following subsections, LL-37 and FF-33 stay as oligomers in PC but dissociate into monomers upon interaction with PS/PC vesicles.

Environment of the NBD moiety in the membrane-bound state of NBD-labelled peptides

The fluorescence emission spectra of NBD-LL-37, NBD-FF-33 and NBD-aminoethanol (used as control), were monitored in PBS and in the presence of vesicles composed of either PC or PC/PS. SUV were used to minimize differential light-scattering effects, and the lipid/peptide molar ratio was elevated ($> 3000:1$) so that the spectral contributions of free peptide would be negligible. In buffer, NBD-labelled peptides and NBD-aminoethanol exhibited a maximum of fluorescence emission at 548 ± 1 nm, which reflects a hydrophilic environment for the NBD moiety [41]. However, when vesicles were added to the aqueous solutions containing NBD-labelled peptides and NBD-aminoethanol, a blue shift in the emission maximum (towards 528 ± 1 nm) and an increase in the fluorescence intensity of the NBD group were observed only with NBD-LL-37 and NBD-FF-33, both in the presence of PC/PS and PC vesicles (results not shown). The change in the spectrum of the NBD group reflects its relocation to a more hydrophobic environment [41]. The blue shifts in the spectra of the NBD-labelled peptides suggest that their N-termini are not penetrating deeply into the hydrophobic region of either PC or PC/PS membranes. Similar blue shifts were observed with other antimicrobial peptides (e.g. dermaseptin and cecropin [28,38,40]) but not with pore-forming polypeptides

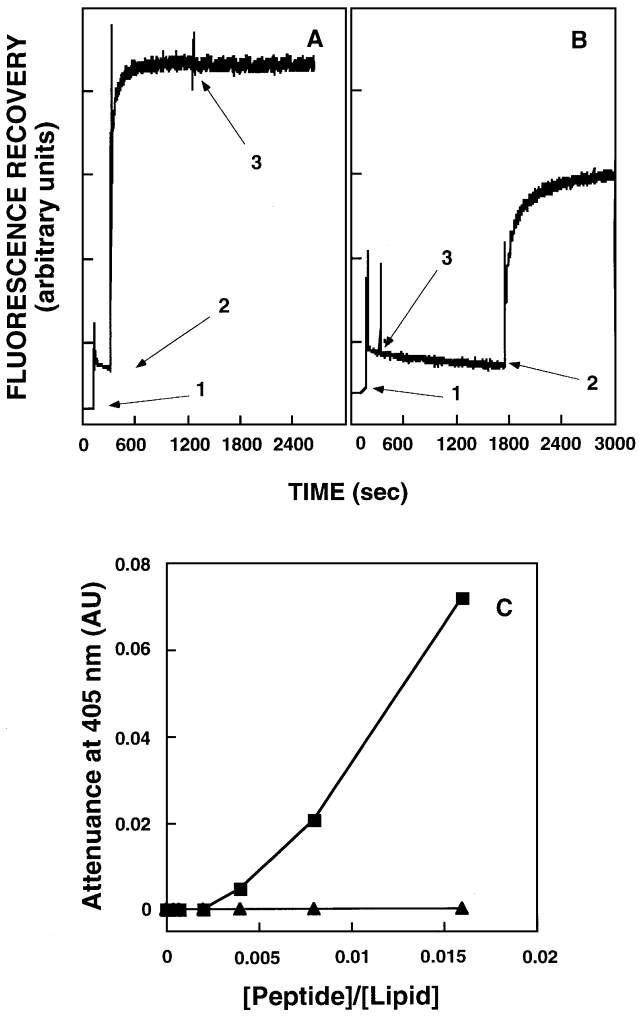

Figure 5 Accessibility of membrane-bound peptides to proteolytic degradation

(**A**) Protection of membrane-bound NBD-labelled LL-37 against proteolytic digestion in the presence of PC/PS vesicles. (**B**) In a control experiment proteinase K was added to NBD-LL-37 in buffer prior to the addition of lipid vesicles. The fluorescence intensity of the labelled peptide was monitored at 530 nm with the excitation set at 470 nm. The digestion was performed in PBS, pH 7.0. 1, 2 and 3 indicate the addition of NBD-LL-37, PC/PS SUV, and proteinase K, respectively. The concentration of NBD-LL-37 was 0.1 μM and that of PC/PS SUV was fixed at 150 μM. (**C**) Detection of aggregation of liposomes mixed with peptides as measured by attenuance changes at 405 nm. LL-37, FF-33, cecropin B, and pardaxin were added to 150 μM SUV composed of PC/cholesterol (10:1 w/w) in PBS. The changes in the attenuance at 405 nm are plotted versus the peptide to lipid molar ratio. LL-37, (▲); Pardaxin, (■). FF-33 and cecropin did not cause aggregation of vesicles and fall on the line of LL-37, and as such the values are not given.

(e.g. pardaxin and the α-5 helix of *Bacillus thuringiensis* δ-endotoxin) which showed emission maxima of 518–525 nm [42].

Vesicle-bound peptides are not susceptible to proteolytic cleavage

NBD-labelled peptides were treated with the proteolytic enzyme proteinase K before and after binding to phospholipid membranes. Figure 5 depicts one such experimental profile for NBD-LL-37 with PS/PC vesicles. In panel A, NBD-labelled peptide was first added to PBS (time point 1), followed by the addition of PS/PC vesicles (time point 2), which caused a large increase in fluorescence. Once the curve reached a plateau, indicating the completion of binding of NBD-labelled peptides to the membrane, proteinase K was added (time point 3) to the peptide–lipid complex. Figure 5(A) shows that, after proteinase K treatment, the fluorescence of the NBD-labelled peptide did not decrease. This indicates that the labelled peptide is not susceptible to degradation in its membrane-bound state. Similar profiles were obtained with PC vesicles (results not shown). Control experiments were done by adding proteinase K to NBD-labelled peptide prior to the addition of vesicles (Figure 5B). When PS/PC vesicles were added (time point 2 of Figure 5B) to the partially degraded peptide, a smaller increase in fluorescence was observed due to binding of the partially uncleaved peptide to vesicles. Similar results were obtained with NBD-FF-33, albeit there was partial degradation, with slow kinetics, in PC vesicles (results not shown). The findings that NBD-LL-37 is protected from degradation when bound to both PC and PS/PC vesicles are different from the results found with other antimicrobial peptides, e.g. cecropins [38,39] and dermaseptins [28,40]. In the latter cases, the antimicrobial peptides were protected from enzymic degradation only when bound to PC/PS vesicles but were completely degraded, with fast kinetics, when bound to PC vesicles.

The ability of LL-37 to induce vesicle aggregation was tested to investigate whether this property was responsible for the peptide's protection from proteolysis. Changes in vesicle size distribution resulting from peptide-induced aggregation can be monitored by following the attenuance of the liposome suspension. The changes in the attenuance at 405 nm as a function of the peptide to lipid molar ratio are shown in Figure 5(C). The results show that LL-37, FF-33 and the antimicrobial peptide cecropin do not cause aggregation of vesicles, whereas the cytotoxic peptide pardaxin [43] causes PC/cholesterol vesicles to aggregate at high peptide to lipid molar ratio. These results were further verified by negative-stain electron microscopy (results not shown).

Organization of the peptides upon binding to zwitterionic and negatively charged vesicles

As shown above, LL-37 and FF-33 oligomerize in solution, therefore they can reach the membrane as monomers and oligomers. To evaluate whether the peptides remain self-associated within membranes and to compare their oligomerization state, the fluorescence of Rho-labelled peptides was monitored in the presence of phospholipid vesicles. When Rho-labelled monomers are associated and their rhodamine probes are in close proximity, the result is self-quenching of the fluorescence emission. Following the addition of PC or PC/PS vesicles, an increase in the fluorescence of both Rho-LL-37 and Rho-FF-33 was observed (Figure 6). Since the fluorescence of rhodamine is only slightly sensitive to the dielectric constant of the medium, this increase of fluorescence is very likely related to a decrease in self-quenching due to the dissociaiton of associated Rho-labelled peptides in the presence of lipid vesicles. The results presented in Figure 6 demonstrate that: (i) fluorescence in the presence of PC/PS vesicles is slightly higher than that of totally cleaved peptides, which is expected if the peptides are completely dissociated upon binding to these membranes; (ii) fluorescence of Rho-labelled peptides in the presence of PC is lower than that in PC/PS vesicles, suggesting that the peptides are partially self-associated when bound to PC membranes; (iii) fluorescence of Rho-LL-37 is lower than that of Rho-FF-33 only in the presence of PC, suggesting that LL-37 exists in a slightly higher oligomeric state when bound to PC membranes. However, the final fluorescence did not reach the level of enzymically cleaved

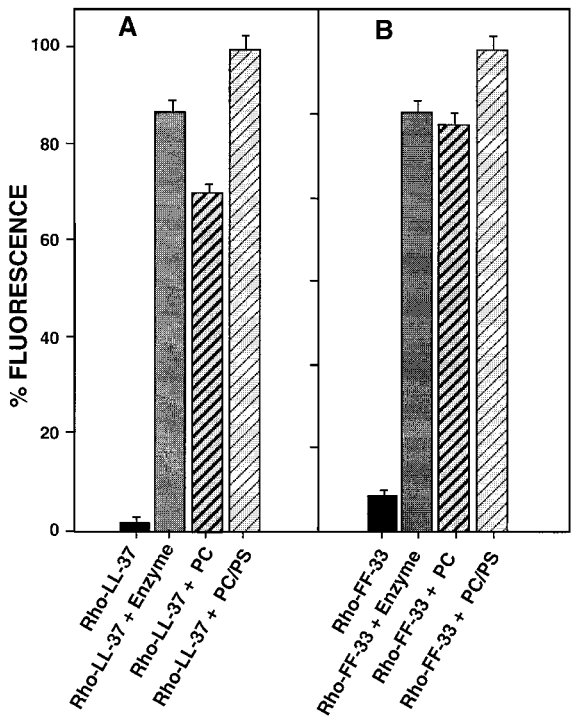

Figure 6 Dissociation of the peptides upon membrane binding

Partial dissociation of Rho-LL-37 and Rho-FF-33 (0.1 μM each) oligomers after binding to PC vesicles (150 μM), third column in (**A**) and (**B**), respectively, and complete dissociation after binding to PC/PS vesicles (150 μM), fourth column in (**A**) and (**B**), respectively. Rhodamine-labelled peptides (0.1 μM) alone (first columns) were treated also with proteinase K to obtain maximal fluorescence of non-membrane bound peptides (second columns). Excitation was set at 530 nm (10 nm slit) and emission was set at 582 nm (8 nm slit).

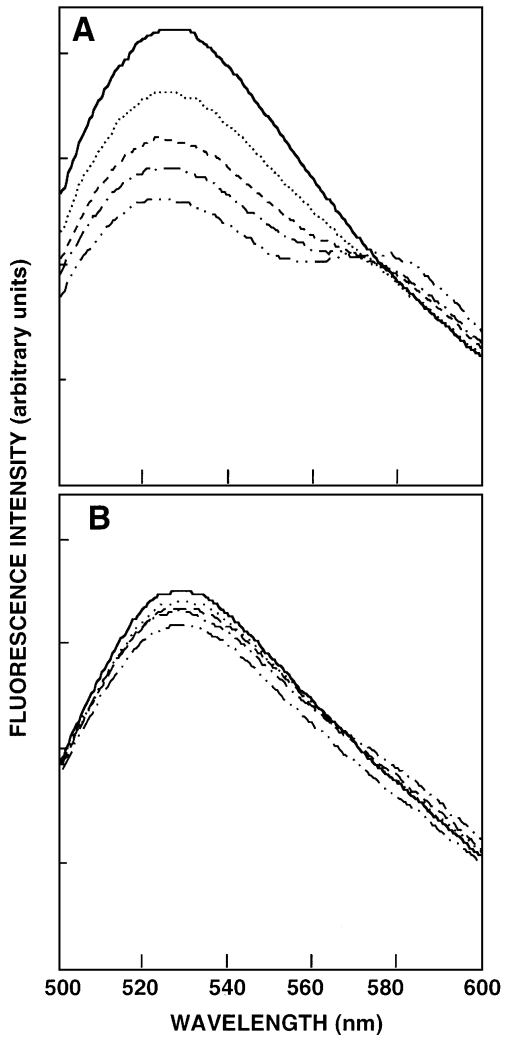

Figure 7 Dependence of fluorescence energy transfer on the Rho-peptide (acceptor) concentration in PC (A) and PC/PS (B) liposomes

The spectra were recorded for the donor-peptide alone and in the presence of various amounts of an acceptor-peptide. The excitation wavelength was set at 460 nm, and the emission scanned from 500 to 600 nm. The liposome concentration was 125 μM. Designations; the spectrum of NBD-LL-37 (0.1 μM) in the presence of SUV alone (——), and with various concentrations of Rho-LL-37; (· · · · · ·) 0.05 μM, (– – – –) 0.1 μM, (–·–·–) 0.15 μM and (–· ·–· ·) 0.25 μM.

rhodamine-labelled peptide which served as a control for completely dissociated peptide (Figure 6). This indicated that the peptides remained self-associated in PC.

To further evaluate whether the observation described above indeed reflected self-association in PC membranes, RET measurements were performed with NBD- and Rho-LL-37 (energy donor and energy acceptor, respectively) as described previously [44]. In the presence of PC phospholipid vesicles (125 μM), addition of Rho-LL-37 (final concentrations of 0.05–0.25 μM) to NBD-LL-37 (0.1 μM) quenched the donor's emission and increased the acceptor's emission, which is consistent with energy transfer (Figure 7A). No energy transfer was observed between NBD-LL-37 and Rho-LL-37 in the presence of PC/PS phospholipid vesicles (Figure 7B). In control experiments, no significant change in the emission spectrum of NBD was observed when equal amounts of unlabelled LL-37 or Rho-cecropin B rather than Rho-LL-37 were added (results not shown).

ATR–Fourier-transform infrared (FTIR) studies

Structure of the peptides in lipid multibilayers as determined by FTIR spectroscopy

FTIR spectroscopy was used to determine the structure of LL-37, FF-33 and their fluorescent derivatives in PC/cholesterol and PC/PG membranes. Helical and unordered residues can contribute to the amide I vibration at almost identical wavenumbers and it is difficult to extract the precise proportion of helix and random coil from IR spectra. However, exchange of hydrogen with ^{2}H makes it possible, in some cases, to differentiate α-helical components from random structure, since the absorption for the latter shifts to a higher extent than for the former after deuteration. Therefore, we examined the IR spectra of the peptide after complete deuteration. Second-derivative analysis showed that the main amide I maximum (80–85%) of all the peptides is centred at 1651 cm^{-1}. This can be attributed to α-helical structure [45]. A smaller component ($\sim$ 15%) appeared at 1625 cm^{-1}, a region which is usually assigned to a β-sheet structure [45]. Another possibility is that this band arises from an extended conformation stabilized by interaction of amino acids with membrane components such as the lipid head groups, and the hydrophobic core of the membrane. Similar spectra were obtained with negatively charged PC/PG membranes and for the fluorescently labelled derivatives, and therefore only the spectra of LL-37 and FF-33 are shown in Figure 8. Deconvolution of the

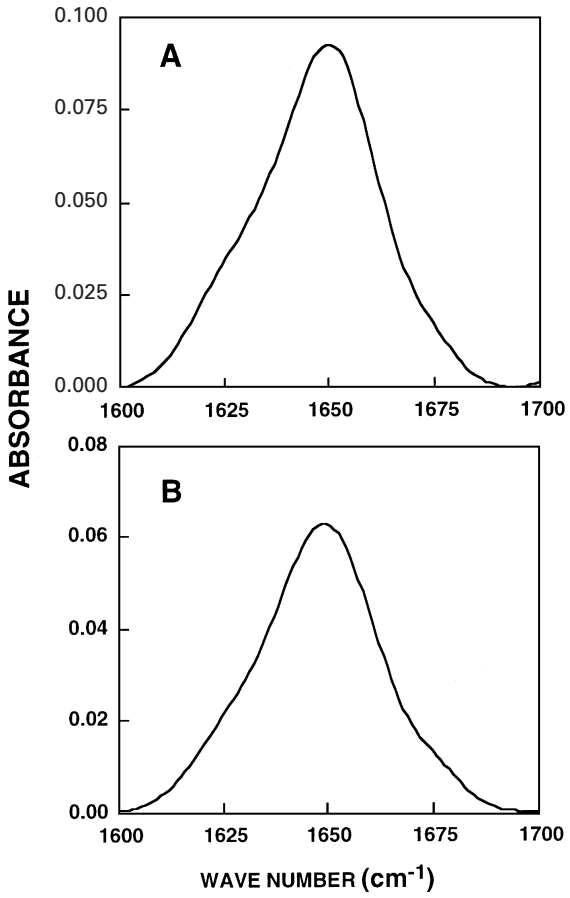

Figure 8 FTIR spectra of the amide I band of the peptides in membranes

FTIR Spectra of the amide I band (1700–1600 cm^{-1}) of (**A**) LL-37 and (**B**) FF-33 in a PC multibilayer. A 80:1 lipid/peptide molar ratio was used. Similar results were obtained with lipid/peptide molar ratios of 120:1 and 40:1.

Table 1 Secondary structures obtained for membrane-bound peptides

A lipid/peptide molar ratio of 80:1 was used. Results are the average of four independent experiments with a S.D. of 4%. Abbreviation: Cho, cholesterol.

Secondary structure (%)				
	PC/Cho		PC/PG	
Sample	α-Helix (1651 cm^{-1})	β-Sheet (1625 cm^{-1})	α-Helix (1651 cm^{-1})	β-Sheet (1625 cm^{-1})
LL-37	85	15	87	13
Rho-LL-37	84	16	87	13
NBD-LL-37	86	14	87	13
FF-33	84	16	84	16
Rho-FF-33	84	16	84	16

amide I region was performed assuming a Gaussian shape for the component peaks and the results are summarized in Table 1. The results revealed similar structures for all the peptides, with a predominantly (80–85%) α-helical structure. The extraction of quantitative information on protein secondary structure from amide I band profiles has been discussed by Surewicz et al. [33].

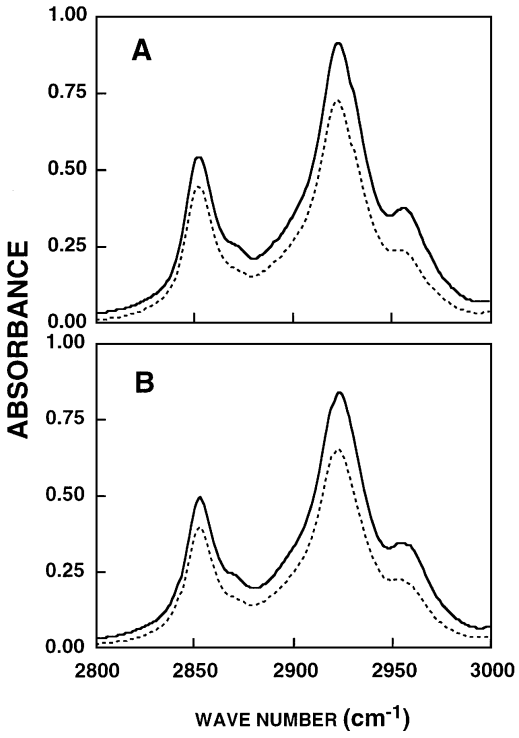

Figure 9 ATR dichroism spectra

ATR dichroism spectra of parallel and perpendicular polarized ATR-FTIR absorbance spectra (3000–2800 cm^{-1}) for the lipid CH_2 symmetric and antisymmetric vibration of PC multibilayers alone (**A**) and incorporated with LL-37 (**B**). The top line is for the P component of polarized incident light (an electric vector oscillates parallel to the ZnSe prism or membrane plane) and the bottom line is for the S (perpendicular) component. The sample was prepared as described in the Experimental section. The lipid/peptide molar ratio was 80:1. Similar results were obtained with lipid/peptide molar ratios of 120:1 and 40:1.

An assumption in this type of quantitative analysis is that the molar absorptions of the amide I bands assigned to different conformers are equal. This assumption may not be correct in all cases [46–48]. However, other studies reported similar intensities for β-stranded and helical polypeptides [47,49], and comparable absorptions were found for β-stranded and random-coiled structures which were obtained from proteins in aqueous solution [50].

Orientation of the phospholipid membranes and the effect of peptide binding on the acyl-chain order

Polarized ATR-FTIR spectroscopy was used to determine the orientation of the lipid membrane. The symmetric [$\nu_{sym}(CH_2) \sim 2850\ cm^{-1}$] and the antisymmetric [$\nu_{antisym}(CH_2) \sim 2930\ cm^{-1}$] vibrations of lipid methylene C–H bonds are perpendicular to the molecular axis of a fully extended hydrocarbon chain. Thus, measurements of the dichroism of IR light absorbance can reveal the order and orientation of the membrane sample relative to the prism surface. Figure 9(A) shows as an example the ATR dichroism spectra of parallel and perpendicular polarized ATR–FTIR absorbance spectra between 2800–3000 cm^{-1} of PC multibilayers. The R^{ATR} values, based on the stronger $\nu_{antisym}(CH_2)$ were 1.23 and 1.37 for PC and PC/PG, respectively. Similar values were obtained when $\nu_{sym}(CH_2)$ was used instead (1.26 and 1.35 for PC and PC/PG, respectively). Based on the dichroic ratio of lipid stretching, the corresponding orientation order

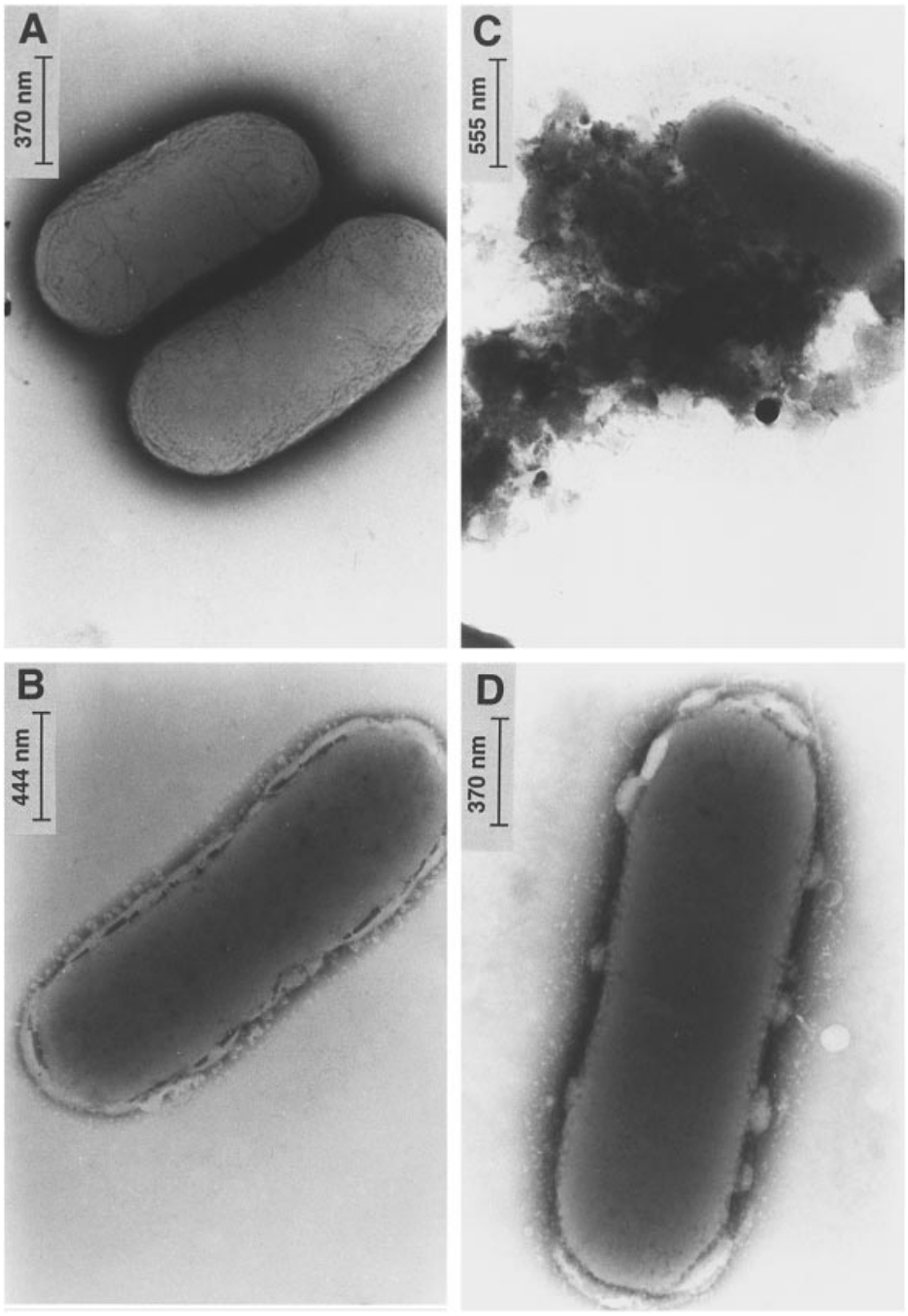

Figure 10 Electron micrographs of negatively stained *E. coli* untreated and treated with LL-37 and cecropin B

(**A**), control; (**B**), after treatment of the bacteria with LL-37 at a concentration lower than the MIC (7.5 μM); (**C**), after treatment of the bacteria with LL-37 at the MIC concentration (12.5 μM); (**D**), after treatment of the bacteria with cecropin B at a concentration lower than the MIC (1 μM).

parameters, f, were calculated to be 0.37 and 0.30 for PC and PC/PG, respectively [based on $\nu_{antisym}(CH_2)$] and 0.35 and 0.31 for PC and PC/PG, respectively [based on $\nu_{\mathrm{sym}}(\mathrm{CH_2})$]. The data indicate that the phospholipid membrane is well ordered, permitting the orientation of the peptides to be determined. Similar results have been reported by others [36,51]. The observed antisymmetric and symmetric peaks at $\sim 2922\,\mathrm{cm^{-1}}$ and $\sim 2853\,\mathrm{cm^{-1}}$, respectively, indicate that the membranes were predominantly in a liquid–crystalline phase [36,52], similarly to what is found in biological cell membranes. Thus, the lipid multibilayers used in our study were well oriented and in a liquid-crystalline phase.

The effect of the peptides on the multibilayer acyl-chain order can be estimated by comparing the $\mathrm{CH_2}$-stretching dichroic ratio of pure phospholipid multibilayers with that obtained for membranes with bound peptides. Similar results were obtained with LL-37 and FF-33 and therefore only results with LL-37 are shown. Figure 9(B) shows as an example the ATR dichroism

spectra of parallel and perpendicular polarized ATR–FTIR absorbance spectra between 2800–3000 cm^{-1} of PC multibilayers containing LL-37. The R^{ATR} values were calculated to be 1.26 and 1.45 for PC and PC/PG, respectively [based on $\nu_{antisym}(CH_2)$], and 1.30 and 1.43 for PC and PC/PG, respectively [based on $\nu_{sym}(CH_2)$]. The corresponding order parameters, *f*, are 0.35 and 0.25 for PC and PC/PG, respectively [based on $\nu_{antisym}(CH_2)$], and 0.33 and 0.26 for PC and PC/PG, respectively [based on $\nu_{sym}(CH_2)$]. The results indicate that incorporation of LL-37 into PC membranes did not significantly change the order of the membrane. These results suggest that LL-37 is surface localized and does not penetrate into the hydrophobic core of the membrane. Thus, the results do not support a model involving channel formation by LL-37.

Orientation of the peptides in lipid multibilayers as determined by ATR-FTIR spectroscopy

Polarized ATR-FTIR spectroscopy was used to determine the orientation of the peptides within lipid bilayers. The dichroic ratio value, R^{ATR}, was calculated from the α-helix amide I absorption in the polarized spectra and found to be 1.25 and 1.32 for PC and PC/PG, respectively. A similar R^{ATR} value was obtained for cecropin P [39]. The corresponding order parameters, *f*, were calculated and found to be -0.26 and -0.23 for PC and PC/PG, respectively. A negative order parameter is typical of helices oriented nearly parallel to the membrane surface [51].

Examination of bacterial lysis by electron microscopy

The effect of LL-37 on the morphology of treated *E. coli* was observed using transmission electron microscopy. In this experiment cecropin B was used as a control. When supplied at their MIC, both peptides caused total lysis of the bacteria (results shown only for LL-37, Figure 10C). However, when the peptides were utilized at concentrations corresponding to 60 % MIC, some differences in the morphology of the treated bacteria were observed. LL-37 caused local perturbations along the whole cell wall (Figure 10B), whereas cecropin B caused large patches (Figure 10D). It should be noted that cecropin B reaches the membrane predominantly as monomers that aggregate on the surface of negatively charged membranes once a threshold concentration has been reached [38], whereas LL-37 reaches the membrane as an oligomer.

DISCUSSION

A wheel projection plot showed that the central part of LL-37 (residues 11–32) could form an amphipathic α-helix, characteristic of membrane permeating peptides, suggesting that this region might have a major role in the toxic activity of the peptides. Here, by using FTIR spectroscopy, we found that both LL-37 and its N-terminal-truncated form, FF-33, adopted an $\sim 85\,\%$ α-helical structure when bound to membranes (Figure 8 and Table 1). These results confirm that the N-terminal region does not contribute significantly to the α-helical structure. Previous studies using CD spectroscopy showed that the α-helical content of LL-37 is also about 50 % in solutions containing ion compositions that mimic those of human plasma, interstitial fluid, and intracellular fluid [26].

Functional studies revealed that LL-37 has several properties which are different from those of native α-helical antimicrobial peptides isolated from invertebrates or vertebrates, and these differences may shed light on its *in vivo* activities. These are: (i) LL-37 oligomerizes in solution and is significantly protected from proteolytic degradation, whereas other native antimicrobial peptides are highly susceptible to enzymic degradation; (ii) it binds and permeates efficiently both zwitterionic and negatively charged phospholipid vesicles compared with native antimicrobial peptides which permeate efficiently only negatively charged membranes; (iii) it is significantly resistant to proteolytic degradation when bound to both zwitterionic and negatively charged phospholipids, whereas native antimicrobial peptides are protected from degradation only when bound to negatively charged membranes; and (iv) it is self-associated when bound to zwitterionic phospholipid vesicles, but dissociates into monomers upon binding to negatively charged vesicles, whereas native antimicrobial peptides are monomeric when bound to both types of membranes. In the following paragraphs these observations will be discussed in more detail.

The fluorescence dequenching experiments using Rho-labelled LL-37 showed that the peptide oligomerizes in an aqueous solution at a very low concentration (0.1 μM), whereas cecropin B (Figure 1), and many other cytolytic peptides, are mostly monomeric at such low concentrations. Chemical cross-linking experiments demonstrated that, depending upon the peptide concentration, LL-37 can exist in aqueous solution as monomers, dimers or trimers (Figure 3). Previous CD and sedimentation equilibrium experiments revealed that, at high concentrations, LL-37 exists as tetramers too [26]. PMAP-37, another α-helical peptide from the cathelicidin family, was also found to oligomerize in aqueous solution at neutral pH [16]. Similarly to other linear amphipathic antimicrobial peptides, LL-37 has a net positive charge, and therefore its ability to oligomerize in solution is quite surprising. One possible explanation may be that the N-terminal part of LL-37 is hydrophobic, containing about 30 % of the hydrophobic amino acids of the peptide, and therefore may serve as a hydrophobic core of the oligomer. In addition, LL-37 contains 5 negative charges which are spread along the peptide chain and which may form salt bridges with the positive charges and therefore stabilize the oligomer. Hydrophobic regions are also found in other cathelicidin peptides, namely, the C-terminus of BMAP-27 and BMAP-28 [17]. Although PMAP-37 does not contain a hydrophobic terminus, it does contain seven negative and nine positive charges along its chain. Other positively charged antimicrobial peptides (e.g. cecropin B, magainin and dermaseptin) which do not oligomerize in solution do not have hydrophobic termini, nor do they have many negatively charged amino acids along the peptide chain. The ability of LL-37 to oligomerize in solution seems to be the major reason for its relative resistance to proteolytic digestion as observed in the fluorescence dequenching experiment (Figure 2B). Support for this hypothesis is our finding that deletion of four amino acids (two of which are hydrophobic) from the N-terminus of LL-37 reduced, to some extent, the level of oligomerization and made the truncated peptide FF-33 more susceptible to enzymic degradation (Figure 2B). The existence of LL-37 in an aggregated as compared with a monomeric state may be advantageous *in vivo*, where resistance to proteolytic digestion in human wounds and blister fluids can influence the life span of the peptide and its efficacy. The haemolytic activity of LL-37 found in the present study, and the cytolytic activity demonstrated in a previous study [26], is common to other amphipathic α-helical members of the cathelicidin family (e.g. PMAP-37 [16], BMAP-27 and BMAP-28 [17]).

The non-cell-specific lytic activity of LL-37 seems to result from its inability to discriminate between zwitterionic PC and negatively charged PC/PS phospholipid membranes (Figure 4), as opposed to non-haemolytic antimicrobial peptides (e.g. derma-

septin S [28], cecropin B2 [38], cecropin P [39], magainin [53] and diastereomers of the cytolytic peptides pardaxin and melittin [54,55]), which could bind and perturb efficiently only negatively charged phospholipid membranes. The major phospholipid component of the hRBC membrane outer leaflet and normal eukaryotic cells is zwitterionic. The high affinity of LL-37 for zwitterionic PC membranes is surprising in light of its high net positive charge (+6). This may suggest the involvement of hydrophobic interactions between the peptide and the vesicles. LL-37 reaches PC membranes as an oligomer (Figure 2) and remains on the membrane as such (Figures 6 and 7). Since the N-terminus of LL-37 is hydrophobic, a bundle of N-terminal regions can initiate binding to the membrane. In addition, some of the positive charges can be neutralized by the negative charges and therefore reduce repulsive forces. In support of this assumption are the findings that, compared with LL-37, FF-33 (which is N-terminally truncated) had less haemolytic activity and was less able to permeate PC membranes. Furthermore, FF-33 had antimicrobial activity identical to that of LL-37, which suggests a role for the central α-helix in antimicrobial but not haemolytic activity. It is possible that further truncation of the N-terminus of LL-37, or substitution of hydrophobic amino acids with hydrophilic ones in the N-terminus, will produce molecules with better selectivity, but further studies are required to address this issue.

LL-37 was also totally protected from enzymic degradation when bound to either PC or PC/PS vesicles (Figure 5). This is in contrast with what has been found with other native antimicrobial peptides. Dermaseptin S1 [28], cecropin B and cecropin P [38,39] are not susceptible to enzymic degradation when bound to PC/PS vesicles, but highly susceptible when bound to PC vesicles. In the case of PC, oligomerization of LL-37 in the membrane may also assist in its stability against degradation, considering the fact that oligomerization prevented degradation even in solution (Figure 1). The reason for its protection is not because it was buried between aggregates of liposomes since it could not cause their aggregation (Figure 5C).

The difference between the morphology of the patches on the bacterial cell wall observed with LL-37 and cecropin B (Figure 10) may relate to their different oligomerization states upon reaching the membrane. LL-37 reaches negatively charged membranes as oligomers and therefore can cause many local perturbations as seen in the electron micrograph (Figure 10).

We have proposed that a non-pore carpet-like mechanism, rather than channel formation via a 'barrel stave' mechanism [42,44], is involved in the membrane-permeating activity of the following antimicrobial peptides: cecropins [32,38,39], dermaseptins S [28] and dermaseptin b [40]. Despite some differences between LL-37 and these antibacterial peptides, it is reasonable to assume that LL-37 acts on membranes via a similar mechanism. Channel formation requires that amphipathic α-helical monomers self-associate and insert into the membrane to form an aqueous pore in which the hydrophilic surface lines the interior of the pore and the hydrophobic surface faces the lipids. We found that, when bound to either zwitterionic PC or negatively charged PC/PS vesicles, the hydrophobic N-terminus of LL-37 is buried only slightly in the membrane as indicated by the extent of NBD blue shift (from an emission maximum at 548 ± 1 nm to 528 ± 1 nm) [41]. Furthermore, LL-37 dissociates into monomers when bound to PC/PS which is in contrast to a channel formation mechanism. Moreover, even when bound to PC as an oligomer (Figures 6 and 7), LL-37 is also surface localized as revealed by ATR-FTIR studies (Figures 8 and 9). In addition, the lethal concentration of LL-37 towards all bacteria tested, and its activity on model phospholipid membranes is similar to that found for cecropins, dermaseptins and diastereomers of lytic peptides, which do not form channels. Scheme 1 shows a model for the various steps presumably involved in the destruction of the two membranes of Gram-negative bacteria. LL-37 reaches the first membrane as oligomers of different size which cause local perturbation followed by dissociation to monomers. Such perturbations were described as a toroidal model [56]. The monomers can easily diffuse to the inner membrane, cover it in a carpet-like manner and disintegrate it too.

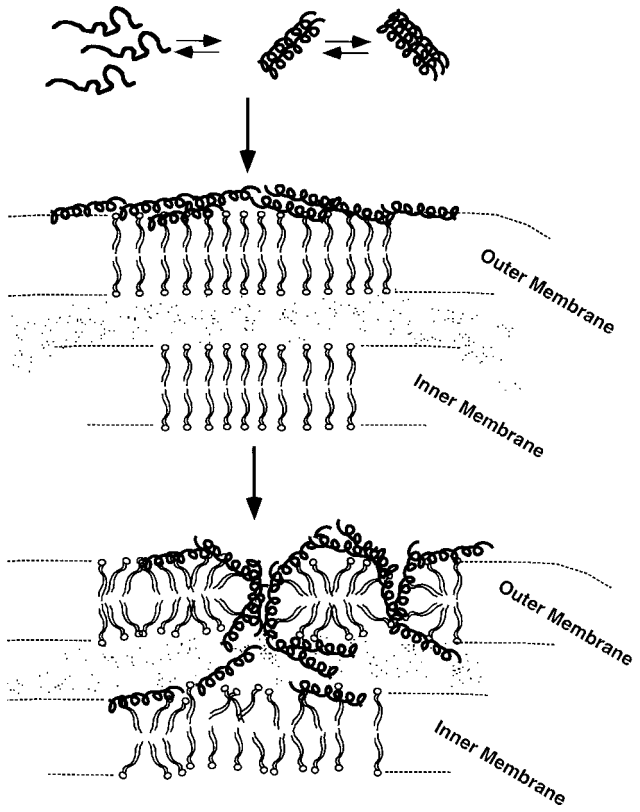

Scheme 1 Model illustrating the action of LL-37 on the cell wall of Gram-negative bacteria

The peptide reaches the outer bacterial membrane as monomers and oligomers of different sizes, and binds to the surface of the membrane causing local perturbation. The oligomers are then dissociated into monomers, which cover the membrane in a carpet-like manner. The monomers diffuse more easily to the inner membrane and disintegrate it, too, after a threshold concentration has been reached.

There is growing evidence that members of the cathelicidin family have functions that extend beyond antimicrobial activity possibly including a role in wound healing [57], chemotaxis and proteinase regulation [58]. LL-37 has been detected in human wounds and blister fluids [24], and more recently the gene coding for LL-37 was found to be induced in human keratinocytes during inflammatory disorders [25]. In addition, LL-37/hCAP18 was found to bind lipopolysaccharide, inhibit its multiple biological activities *in vitro* and reduce its lethality in murine models of endotoxaemia [59]. All this evidence, including the fact that LL-37 can interact with the eukaryotic cell membrane, may indicate that LL-37 plays important extracellular roles in inflammation and wound healing in addition to its role in the human immune system. Further studies are required to determine the activity of LL-37 *in vivo*. Combining information on mechanism

and activity may lead to development of LL-37 and related peptides as potential drugs in the treatment of wounds and inflammations.

This research was supported in part by the Basic Research Foundation administered by the Israel Academy of Sciences and Humanities, and the Swedish Medical Research Council.

REFERENCES

1 Nicolas, P. and Mor, A. (1995) Annu. Rev. Microbiol. **49**, 277–304
2 Boman, H. G. (1995) Annu. Rev. Immun. **13**, 61–92
3 Ritonja, A., Kopitar, M., Jerala, R. and Turk, V. (1989) FEBS Lett. **255**, 211–214
4 Zanetti, M., Gennaro, R. and Romeo, D. (1995) FEBS Lett. **374**, 1–5
5 Agerberth, B., Lee, J. Y., Bergman, T., Carlquist, M., Boman, H. G., Mutt, V. and Jornvall, H. (1991) Eur. J. Biochem. **202**, 849–854
6 Storici, P. and Zanetti, M. (1993) Biochem. Biophys. Res. Commun. **196**, 1058–1065
7 Gennaro, R., Skerlavaj, B. and Romeo, D. (1989) Infect. Immun. **57**, 3142–3146
8 Bagella, L., Scocchi, M. and Zanetti, M. (1995) FEBS Lett. **376**, 225–228
9 Mahoney, M. M., Lee, A. Y., Brezinski-Caliguri, D. J. and Huttner, K. M. (1995) FEBS Lett. **377**, 519–522
10 Tossi, A., Scocchi, M., Skerlavaj, B. and Gennaro, R. (1994) FEBS. Lett, **339**, 108–112
11 Gallo, R. L., Kim, K. J., Bernfield, M., Kozak, C. A., Zanetti, M., Merluzzi, L. and Gennaro, R. (1997) J. Biol. Chem. **272**, 13088–13093
12 Agerberth, B., Gunne, H., Odeberg, J., Kogner, P., Boman, H. G. and Gudmundsson, G. H. (1995) Proc. Natl. Acad. Sci. U.S.A. **92**, 195–199
13 Scocchi, M., Skerlavaj, B., Romeo, D. and Gennaro, D. (1992) Eur. J. Biochem. **209**, 589–595
14 Zanetti, M., Litteri, L., Griffiths, G., Gennaro, R. and Romeo, D. (1991) J. Immunol. **146**, 4295–4300
15 Storici, P., Scocchi, M., Tossi, A., Gennaro, R. and Zanetti, M. (1994) FEBS Lett. **337**, 303–307
16 Tossi, A., Scocchi, M., Zanetti, M., Storici, P. and Gennaro, R. (1995) Eur. J. Biochem. **228**, 941–946
17 Skerlavaj, B., Gennaro, R., Bagella, L., Merluzzi, L., Risso, A. and Zanetti, M. (1996) J. Biol. Chem. **271**, 28375–28381
18 Skerlavaj, B., Romeo, D. and Gennaro, R. (1990) Infect. Immun. **58**, 3724–3730
19 Boman, H. G., Agerberth, B. and Boman, A. (1993) Infect. Immun. **61**, 2978–2984
20 Gudmundsson, G. H., Agerberth, B., Odeberg, J., Bergman, T., Olsson, B. and Salcedo, R. (1996) Eur. J. Biochem. **238**, 325–332
21 Larrick, J. W., Hirata, M., Shimomoura, Y., Yoshida, M., Zheng, H., Zhong, J. and Wright, S. C. (1993) Antimicrob. Agents Chemother. **37**, 2534–2539
22 Gudmundsson, G. H., Magnusson, K. P., Chowdhary, B. P., Johansson, M., Andersson, L. and Boman, H. G. (1995) Proc. Natl. Acad. Sci. U.S.A. **92**, 7085–7089
23 Segrest, J. P., De-Loof, H., Dohlman, J. G., Brouillette, C. G. and Anantharamaiah, G. M. (1990) Proteins **8**, 103–117
24 Frohm, M., Gunne, H., Bergman, A. C., Agerberth, B., Bergman, T., Boman, A., Liden, S., Jornvall, H. and Boman, H. G. (1996) Eur. J. Biochem. **237**, 86–92
25 Frohm, M., Agerberth, B., Ahangari, G., Stahle-Backdahl, M., Liden, S., Wigzell, H. and Gudmundsson, G. H. (1997) J. Biol. Chem. **272**, 15258–15263
26 Johansson, J., Gudmundsson, G. H., Rottenberg, M. E., Berndt, K. D. and Agerberth, B. (1998) J. Biol. Chem. **273**, 3718–3724
27 Merrifield, R. B., Vizioli, L. D. and Boman, H. G. (1982) Biochemistry **21**, 5020–5031
28 Pouny, Y., Rapaport, D., Mor, A., Nicolas, P. and Shai, Y. (1992) Biochemistry **31**, 12416–12423
29 Bartlett, G. R. (1959) J. Biol. Chem. **234**, 466–468
30 Schagger, H. and Jagow, G. V. (1987) Anal. Biochem. **166**, 368–379
31 Shai, Y., Bach, D. and Yanovsky, A. (1990) J. Biol. Chem. **265**, 20202–20209
32 Gazit, E., Miller, I. R., Biggin, P. C., Sansom, M. S. and Shai, Y. (1996) J. Mol. Biol. **258**, 860–870
33 Surewicz, W. K., Mantsch, H. H. and Chapman, D. (1993) Biochemistry **32**, 389–394
34 Krimm, S. and Bandekar, J. (1986) Adv. Protein Chem. **38**, 181–364
35 Harrick, N. J. (1967) Internal Reflection Spectroscopy, Wiley, New York
36 Ishiguro, R., Kimura, N. and Takahashi, S. (1993) Biochemistry **32**, 9792–9797
37 Rothschild, K. J. and Clark, N. A. (1979) Science **204**, 311–312
38 Gazit, E., Lee, W. J., Brey, P. T. and Shai, Y. (1994) Biochemistry **33**, 10681–10692
39 Gazit, E., Boman, A., Boman, H. G. and Shai, Y. (1995) Biochemistry **34**, 11479–11488
40 Strahilevitz, J., Mor, A., Nicolas, P. and Shai, Y. (1994) Biochemistry **33**, 10951–10960
41 Chattopadhyay, A. and London, E. (1987) Biochemistry **26**, 39–45
42 Gazit, E. and Shai, Y. (1993) Biochemistry **32**, 12363–12371
43 Shai, Y., Fox, J., Caratsch, C., Shih, Y. L., Edwards, C. and Lazarovici, P. (1988) FEBS Lett. **242**, 161–166
44 Rapaport, D. and Shai, Y. (1992) J. Biol. Chem. **267**, 6502–6509
45 Jackson, M. and Mantsch, H. H. (1995) Crit. Rev. Biochem. Mol. Biol. **30**, 95–120
46 Jackson, M., Haris, P. I. and Chapman, D. (1989) Biochim. Biophys. Acta **998**, 75–79
47 Venyaminov, S. Y. and Kalnin, N. N. (1990) Biopolymers **30**, 1259–1271
48 Harmen, H. J. de J., Goormaghtigh, E. and Ruysschaert, J. M. (1996) Anal. Biochem. **242**, 95–103
49 Chirgadze, Y. N. and Brazhnikov, E. V. (1974) Biopolymers **13**, 1701–1712
50 Chirgadze, Y. N., Shestopalov, B. V. and Vanyaminou, S. Y. (1973) Biopolymers **12**, 1337–1351
51 Tamm, L. K. and Tatulian, S. A. (1997) Q. Rev. Biophys. **30**, 365–429
52 Cameron, D. G., Casal, H. L., Gudgin, E. F. and Mantsch, H. H. (1980) Biochim. Biophys. Acta **596**, 463–467
53 Schumann, M., Dathe, M., Wieprecht, T., Beyermann, M. and Bienert, M. (1997) Biochemistry **36**, 4345–4351
54 Shai, Y. and Oren, Z. (1996) J. Biol. Chem. **271**, 7305–7308
55 Oren, Z. and Shai, Y. (1997) Biochemistry **36**, 1826–1835
56 Matsuzaki, K., Murase, O., Fujii, N. and Miyajima, K. (1995) Biochemistry **34**, 6521–6526
57 Gallo, R. L., Ono, M., Povsic, T., Page, C., Eriksson, E., Klagsbrun, M. and Bernfield, M. (1994) Proc. Natl. Acad. Sci. U.S.A. **91**, 11035–11039
58 Verbanac, D., Zanetti, M. and Romeo, D. (1993) FEBS Lett. **317**, 255–258
59 Larrick, J. W., Hirata, M., Balint, R. F., Lee, J., Zhong, J. and Wright, S. C. (1995) Infect. Immun. **63**, 1291–1297

Received 14 January 1999/6 April 1999; accepted 13 May 1999